20th Australasian Fluid Mechanics Conference
Perth, Australia
5-8 December 2016

Effects of Partial Slip on Rotating-Disc Boundary-Layer Flows

S. O. Stephen

School of Mathematics and Statistics
University of Sydney, Sydney NSW 2006, Australia

Abstract

An asymptotic study is presented for the effects of partial slip on the linear stability of the flow due to a rotating disc to take into account the effect of surface roughness. The basic steady flow is obtained as an exact solution of the Navier-Stokes equations. The linear stability of this flow for perturbations corresponding to stationary crossflow vortices is considered for the inviscid Type I instabilities by considering the appropriate asymptotic regimes. Predictions for the neutral wavenumbers and orientations of the crossflow vortices are obtained.

Introduction

The asymptotic study of Hall [9] revealed the structure of instability modes in the flow due to a rotating disc. He considered stationary disturbances, rotating with the disc, which take the form of co-rotating vortices. He found that there are two neutrally stable modes; one governed by inviscid mechanisms and the other by viscous mechanisms, corresponding, respectively, to the upper and lower branches of the neutral stability curve. These modes have subsequently been designated as Type I and Type II modes.

Of interest are the stationary crossflow vortices which arise in the transition process from a laminar to a turbulent flow. The present study determines the important instability mechanisms at large Reynolds numbers when the no-slip boundary condition is replaced by a partial-slip condition.

Recent studies have investigated the stability of the flow over a rough rotating disc, motivated by the potential for drag reduction. The numerical study of Cooper *et al.* [2] has shown the effects of partial-slip boundary conditions on the Type I and Type II instabilities for flow over a rotating disc. The partial-slip condition approximates the no-slip boundary condition for the case of small-scale roughness compared to the boundary-layer thickness. It was found that the Type I instability was stabilised for both anisotropic and isotropic roughness. The effect on the Type II instabilities is of particular interest here as Cooper *et al.* [2] show that it can be destabilising. An energy analysis was also conducted to determine the dominant physical mechanisms.

A subsequent study by Garrett *et al.* [5] investigated the effect of an alternative formulation for the roughness for the linear stability of flow due to a rotating disc with surface roughness. Similar results were found compared to the case of partial-slip considered by Cooper *et al.* [2] for the Type I modes, but differences were obtained for the Type II modes.

The study of Cooper *et al.* [2] has been extended by Alveroglu *et al.* [1] to consider the effect of surface roughness on the BEK family of flows (Bodewadt and Ekman layer flows as well as von Kármán flows).

The effects of partial slip on a non-Newtonian Reiner–Rivlin fluid were considered by [11]. Non-Newtonian flows due to a rotating disc have many industrial applications. Previous studies have determined the numerical solutions for various fluids (see the review paper by [10] and the recent results of [3] for a power-law fluid). The first linear stability analyses of such flows has been given by [6, 7, 8].

This study is the first asymptotic investigation of the boundary-layer flow over a slip surface. We consider the linear stability of the inviscid (Type I) modes for flow due to a rough rotating disc. The solutions for the disturbed flow are determined in the appropriate asymptotic regimes for large values of the Reynolds number. These provide predictions for the wavenumber and wave angle of the neutral disturbances. Solutions are presented for a particular anisotropic roughness. Conclusions are drawn as to the significance of the results in relation to drag reduction. Finally, ongoing and future directions are discussed.

Formulation

We consider the effect of roughness on the stability of the flow due to a rotating disc, following the approach of [2] and imposing a partial-slip boundary condition at the wall. Anisotropic and isotropic roughnesses are able to be modelled in this way.

The flow of an incompressible fluid of viscosity ν due to a rotating disc is considered. If Ω is the angular rotation of the disc and l is a typical length scale of the problem, we define the Reynolds number $Re = \Omega l^2/\nu$, which will be considered large in the analysis to follow. We non-dimensionalise the governing equations with respect to l, with the velocity scale Ωl and use (non-dimensional) cylindrical polar coordinates (r, θ, z), rotating with the disc. The basic steady flow, obtained as an exact solution of the continuity and Navier–Stokes equations, is $\mathbf{u_B} = [r\bar{u}(\zeta), r\bar{v}(\zeta), Re^{-1/2}\bar{w}(\zeta)]$, where $\zeta = Re^{1/2}z$. The functions $\bar{u}$, $\bar{v}$ and $\bar{w}$ satisfy the von Kármán equations with partial-slip boundary conditions, namely

$$2\bar{u} + \bar{w}' = 0, \quad (1)$$

$$\bar{u}^2 - (\bar{v}+1)^2 + \bar{u}'\bar{w} - \bar{u}'' = 0, \quad (2)$$

$$2\bar{u}(\bar{v}+1) + \bar{v}'\bar{w} - \bar{v}'' = 0, \quad (3)$$

subject to

$$\bar{u}(0) = \lambda\bar{u}'(0), \quad \bar{v}(0) = \eta\bar{v}'(0) \quad \text{and} \quad \bar{w}(0) = 0, \quad (4)$$

$$\bar{u} \to 0, \quad \bar{v} \to -1 \quad \text{as} \quad \zeta \to \infty. \quad (5)$$

Here a prime denotes differentiation with respect to ζ and the coefficients λ and η give a measure of the roughness in the radial and azimuthal directions, respectively. We can consider two types of anisotropic roughnesses on the rotating disc. If $\lambda = 0$ and $\eta > 0$ this corresponds to concentric grooves. If $\lambda > 0$ and $\eta = 0$ this corresponds to radial grooves. We can consider isotropic roughness for when $\lambda = \eta > 0$. An example of the basic flow solutions $\bar{u}$, $\bar{v}$ and $\bar{w}$ is shown in figure 1 for anisotropic roughness with $\lambda = 0.25$ and $\eta = 0$.

We proceed to carry out a linear stability analysis for perturbations corresponding to stationary crossflow vortices. The inviscid Type I instability is investigated by considering the appropriate asymptotic regimes. This is an extension of the study of [9] to consider the effect of roughness.

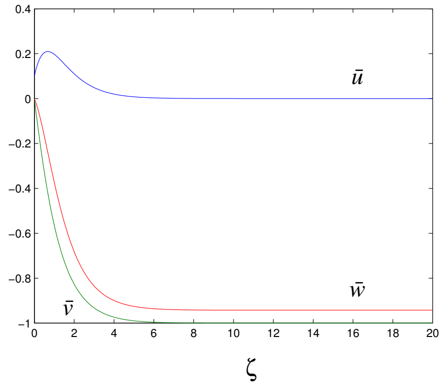

Figure 1: The basic flow solutions $\bar{u}$, $\bar{v}$ and $\bar{w}$ as functions of ζ for $\lambda = 0.25$ and $\eta = 0$.

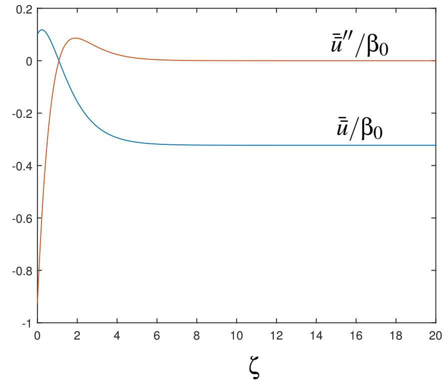

Figure 2: Graphs of $\bar{\bar{u}}/\beta_0$ and $\bar{\bar{u}}''/\beta_0$ as functions of ζ for $\lambda = 0.25$ and $\eta = 0$.

Inviscid modes

The linear stability problem is considered, following the analysis of [9]. We consider the perturbed flow $\mathbf{u} = \mathbf{u_B} + \mathbf{U}$. For large Reynolds number the boundary-layer thickness is $\delta = Re^{-1/2}$. We introduce the small parameter $\varepsilon = Re^{-1/6}$ and consider disturbances proportional to

$$E = \exp\left[\frac{\mathrm{i}}{\varepsilon^3}\left(\int^r \alpha(r,\varepsilon)\,\mathrm{d}r + \theta\beta(\varepsilon)\right)\right].$$

The partial-slip boundary conditions lead to a different asymptotic structure compared to that detailed in [9] for the no-slip case. The wavenumbers α and β expand as

$$\alpha = \alpha_0 + \varepsilon^{3/2}\alpha_1 + \cdots, \quad (6)$$
$$\beta = \beta_0 + \varepsilon^{3/2}\beta_1 + \cdots. \quad (7)$$

The inviscid zone comprises the boundary layer so is of thickness $O(\varepsilon^3)$. The velocity perturbations are given by $U = u(r,z)E$ where $u = u_0(\zeta) + \varepsilon^{3/2}u_1(\zeta) + \cdots$ and similarly, for V, W and P.

Substituting the disturbed flow into the governing equations, yields at leading order an equation for the leading-order normal velocity perturbation, w_0, namely

$$\bar{\bar{u}}\left(w_0'' - \gamma_0^2 w_0\right) - \bar{\bar{u}}'' w_0 = 0, \quad (8)$$

subject to

$$w_0 = 0 \quad \text{at} \quad \zeta = 0 \quad \text{and} \quad w_0 \to 0 \quad \text{as} \quad \zeta \to \infty. \quad (9)$$

Here $\bar{\bar{u}} = \alpha_0\bar{u}r + \beta_0\bar{v}$ is the effective velocity and $\gamma_0^2 = \alpha_0^2 + \beta_0^2/r^2$. In the same way as for the no-slip case of [9] we find that at a value of $\zeta = \bar{\zeta}$ we have $\bar{\bar{u}}$ and $\bar{\bar{u}}''$ are both zero. Thus, equation (8) does not have a singularity at $\zeta = \bar{\zeta}$. This leads to $\alpha_0 r/\beta_0 = -\bar{v}(\bar{\zeta})/\bar{u}(\bar{\zeta})$. Equation (8) can be solved numerically (using finite differences) for the eigenvalue γ_0^2 for particular values of the slip coefficients λ and η.

As an example, figure 2 shows the location of the critical value $\zeta = \bar{\zeta} \approx 1.079$ for $\lambda = 0.25$ and $\eta = 0$, which corresponds to $\alpha_0 r/\beta_0 \approx 3.10$. The corresponding solution for w_0 is shown in figure 3, where $\gamma_0 \approx 0.647$.

A wall layer of thickness $O(\varepsilon^{9/2})$ is required to satisfy the partial-slip wall boundary conditions. The analysis and solutions in the wall layer differ from those in [9] so are given in

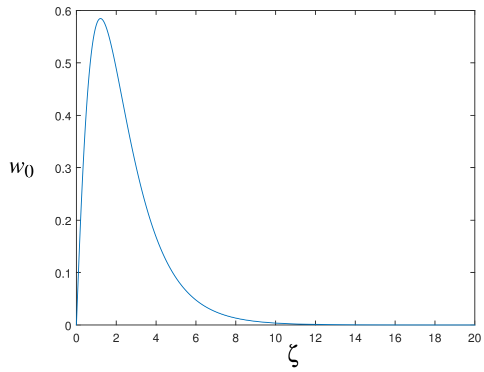

Figure 3: The solution for $w_0(\zeta)$ for $\lambda = 0.25$ and $\eta = 0$.

detail. In particular, the pressure disturbance is larger. Defining $\xi = \varepsilon^{-9/2}z$, then in the wall layer the velocity and pressure perturbations expand as

$$u = U_0(\xi) + \varepsilon^{3/2}U_1(\xi) + \cdots, \quad (10)$$
$$v = V_0(\xi) + \varepsilon^{3/2}V_1(\xi) + \cdots, \quad (11)$$
$$w = \varepsilon^{3/2}W_0(\xi) + \cdots, \quad (12)$$
$$P = P_c(\xi) + \varepsilon^{3/2}P_0(\xi) + \cdots, \quad (13)$$

while the basic flow quantities have the forms

$$\bar{u} = \bar{u}_w + \varepsilon^{3/2}\xi\bar{u}'(0) + \cdots,$$
$$\bar{v} = \bar{v}_w + \varepsilon^{3/2}\xi\bar{v}'(0) + \cdots,$$
$$\bar{w} = \varepsilon^{3/2}\xi\bar{w}'(0) + \cdots.$$

Here $\bar{u}_w = \bar{u}(0)$ and $\bar{v}_w = \bar{v}(0)$. Satisfying the linear disturbance equations, the boundary conditions and matching with the inviscid solution yields the following solutions at leading order

$$U_0 = \frac{\mathrm{i}\alpha_0 w_0'(0)}{\gamma_0^2}\left(1 - e^{-\sigma\xi}\right), \quad (14)$$
$$V_0 = \frac{\mathrm{i}\beta_0 w_0'(0)}{r\gamma_0^2}\left(1 - e^{-\sigma\xi}\right), \quad (15)$$
$$W_0 = w_0'(0)\xi - \frac{w_0'(0)}{\sigma}\left(1 - e^{-\sigma\xi}\right), \quad (16)$$

and $P_c = -\mathrm{i}\bar{\bar{u}}_w w_0'(0)/\gamma_0^2$, where $\sigma = \sqrt{\mathrm{i}\bar{\bar{u}}_w}$, taking the positive real part. Here $\bar{\bar{u}}_w = r\alpha_0\bar{u}_w + \beta_0\bar{v}_w$, and is positive for anisotropic roughness with $\lambda > 0$ and $\eta = 0$.

The analysis in the inviscid zone must be continued to the next order to find the first-order corrections to the wavenumbers. We find w_1 satisfies the same inhomogeneous equation as determined by Hall [9], namely

$$\bar{\bar{u}}\left(w_1'' - \gamma_0^2 w_1\right) - \bar{\bar{u}}'' w_1 = 2\bar{\bar{u}}\left(\alpha_0\alpha_1 + \frac{\beta_0\beta_1}{r^2}\right) w_0 + \left(\alpha_1 - \frac{\beta_1\alpha_0}{\beta_0}\right) r\left(\bar{u}'' - \frac{\bar{\bar{u}}''\bar{u}}{\bar{\bar{u}}}\right) w_0. \tag{17}$$

Solving this equation and matching with the solution in the wall layer leads to the eigenrelation

$$2\left(\alpha_0\alpha_1 + \frac{\beta_0\beta_1}{r^2}\right) I_1 + \left(\frac{\alpha_1}{\beta_0} - \frac{\beta_1\alpha_0}{\beta_0^2}\right) r I_2 = -\frac{(w_0'(0))^2}{\sigma}. \tag{18}$$

Here

$$I_1 = \int_0^\infty w_0^2(t)\,\mathrm{d}t, \tag{19}$$

and

$$I_2 = \beta_0 \int_0^\infty w_0^2 \left(\frac{\bar{u}''\bar{\bar{u}} - \bar{\bar{u}}''\bar{u}}{\bar{\bar{u}}^2}\right) \mathrm{d}t. \tag{20}$$

Note that the integration for I_2 must be deformed above (below) the singularity at $\zeta = \bar{\zeta}$ if $\bar{\bar{u}}'(\bar{\zeta}) < 0\ (> 0)$.

Results

The eigenrelation (18) allows solutions for $\alpha_0\alpha_1 + \beta_0\beta_1/r^2$ and $\alpha_1/\beta_0 - \beta_1\alpha_0/\beta_0^2$ to be obtained, which can be used to determine the first-order corrections to the effective wavenumber and orientation of the vortices. We find that

$$\alpha_0\alpha_1 + \frac{\beta_0\beta_1}{r^2} = \frac{\gamma_c}{r^{1/2}}$$

and

$$\frac{\alpha_1}{\beta_0} - \frac{\beta_1\alpha_0}{\beta_0^2} = \frac{\phi_c}{r^{1/2}},$$

where γ_c and ϕ_c are constants depending on the basic flow solution and the leading order solution, for particular values of slip coefficients λ and η. When $\bar{\bar{u}}_w > 0$, if we write $\bar{u}_c = \bar{u}(\bar{\zeta})$, $\bar{v}_c = \bar{v}(\bar{\zeta})$, $I_2 = I_{2r} + \mathrm{i}I_{2i}$ and $\sigma = \sqrt{\mathrm{i}\bar{\bar{u}}_w} = r^{1/2}\sigma_c(1+\mathrm{i})$, where σ_c is a constant given by

$$\sigma_c = \frac{\gamma_0^{1/2}}{\sqrt{2}(1+\bar{v}_c^2/\bar{u}_c^2)^{1/4}}\left(\bar{v}_w - \frac{\bar{v}_c\bar{u}_w}{\bar{u}_c}\right)^{1/2},$$

then we have

$$\gamma_c = -\frac{(w_0'(0))^2}{4I_1\sigma_c}\left(1 + \frac{I_{2r}}{I_{2i}}\right) \tag{21}$$

and

$$\phi_c = \frac{(w_0'(0))^2}{2\sigma_c I_{2i}}. \tag{22}$$

Define the Reynolds number based on the boundary-layer thickness as R_δ so we have $R_\delta = Re^{1/2}r$ for the rotating disc. Thus, the effective wavenumber of the disturbance, k_δ, becomes

$$\begin{aligned} k_\delta = \sqrt{\alpha^2 + \frac{\beta^2}{r^2}} &= \gamma_0 + \frac{\varepsilon^{3/2}}{\gamma_0}\left(\alpha_0\alpha_1 + \frac{\beta_0\beta_1}{r^2}\right) + \cdots \\ &= \gamma_0 + \frac{\varepsilon^{3/2}}{r^{1/2}}\frac{\gamma_c}{\gamma_0} + \cdots \\ &= \gamma_0 + \frac{\gamma_c}{\gamma_0}\frac{Re^{-1/4}}{r^{1/2}} + \cdots \\ &= \gamma_0 + \frac{\gamma_c}{\gamma_0}R_\delta^{-1/2} + \cdots. \end{aligned} \tag{23}$$

The orientation of the vortices is described by the wave angle ϕ, where ϕ denotes the angle between the normal to the radius vector and the tangent of the spiral. We have

$$\begin{aligned} \tan\left(\frac{\pi}{2} - \phi\right) &= \frac{r\alpha_0}{\beta_0} + \varepsilon^{3/2} r\left(\frac{\alpha_1}{\beta_0} - \frac{\beta_1\alpha_0}{\beta_0^2}\right) + \cdots \\ &= \frac{r\alpha_0}{\beta_0} + \frac{\varepsilon^{3/2}}{r^{1/2}}\phi_c + \cdots \\ &= \frac{r\alpha_0}{\beta_0} + \phi_c\frac{Re^{-1/4}}{r^{1/2}} + \cdots \\ &= \frac{r\alpha_0}{\beta_0} + \phi_c R_\delta^{-1/2} + \cdots. \end{aligned} \tag{24}$$

In these forms the predictions for the neutral wavenumbers and orientations of the crossflow vortices can be compared with numerical results, for instance those of [2] for anisotropic and isotropic roughness.

In the first instance, here these results can be compared to the case of no-slip; the corrected results of [9] given by Gajjar [4]. These are

$$k_\delta = \sqrt{\alpha^2 + \frac{\beta^2}{r^2}} = 1.16 - 9.1R_\delta^{-1/3} + \cdots, \tag{25}$$

and

$$\tan\left(\frac{\pi}{2} - \phi\right) = 4.26 + 17.4R_\delta^{-1/3} + \cdots. \tag{26}$$

Note the different dependance on R_δ for the partial-slip case.

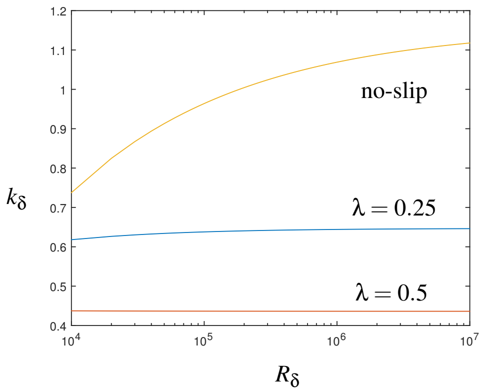

Figure 4: The approximation to the effective wavenumber k_δ from (23) with $\eta = 0$ for $\lambda = 0.25, 0.5$ and for the no-slip result (25).

Figure 4 shows the results using the first two terms from equation (23) for the effective wavenumber, k_δ, of the neutral disturbances for values of the slip coefficients $\eta = 0$ and two values of λ, namely $\lambda = 0.25$ and $\lambda = 0.5$. We find that for partial slip the values are lower than those for the no-slip case, equation (25) also shown. These curves correspond to the upper branch of the neutral stability curve, so the flow is unstable for values below the curve. Thus, these modes are stabilised in the case of partial slip as the range of unstable wavenumbers is reduced.

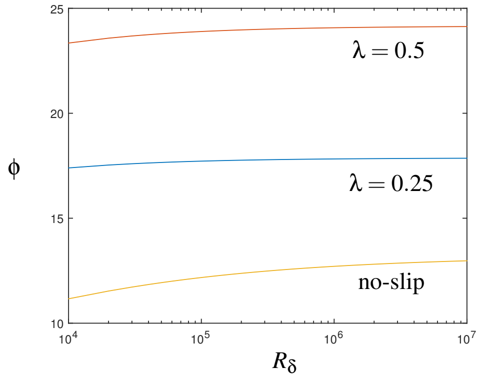

Figure 5: The approximation to the wave angle ϕ from (24) with $\eta = 0$ for $\lambda = 0.25, 0.5$ and for the no-slip result (26).

Figure 5 shows the approximation for the wave angle, ϕ, of the disturbances using the first two terms of equation (24) for values of the slip coefficients corresponding to figure 4 and equation (26) for the case of no-slip. Here the flow is unstable above the curves. We see that the wave angle in the case of partial wall-slip is larger than the no-slip case. This corresponds to a larger number of vortices.

Conclusions

Our analysis has been able to elucidate the asymptotic structure of a boundary-layer flow with partial-slip boundary conditions for the case $\lambda > 0$ and $\eta = 0$. The asymptotic structure for the rotating disc is altered, with a significant increase in the pressure. In, particular, we have demonstrated that inviscid modes (Type I) corresponding to co-rotating vortices exist in rotating flows with partial-slip boundary conditions. The results of this asymptotic study have furthered the knowledge of how roughness may be used for drag reduction in rotating flows.

Our results are in agreement with those of Cooper *et al.* [2], who found that Type I modes are stabilised for a rough surface.

The basic flow solutions obtained for anisotropic roughness with $\lambda = 0$ and $\eta > 0$ reveal that the effective velocity profile is negative at the wall. Thus, there may be zero, one or two critical layers and the analysis presented is not valid for this case. Further investigations are required to asertain the structure of the instability modes for this wall boundary condition, corresponding to concentric grooves. Investigations are currently underway for the case of isotropic roughness, i.e. when $\lambda \neq 0$ and $\eta \neq 0$.

Since [2] found that the effect of roughness on the Type II modes can be destabilising, it is of interest to determine the asymptotic structure of these viscous modes. Ongoing work is investigating the effect of no-slip boundary conditions on the Type II instability mode and we hope to report on this shortly.

Another avenue of current focus is the effect of partial slip on the basic flows of several types of non-Newtonian rotating-disc flow. The first linear stability analyses of non-Newtonian flows with partial-slip boundary conditions will also be considered using asymptotic methods for large Reynolds numbers.

Acknowledgements

The author acknowledges useful discussions with Professor S. J. Garrett.

References

[1] Alveroglu, B., Segalini, A. and Garrett, S.J., The effect of surface roughness on the convective instability of the BEK family of boundary-layer flows, *Eur. J. Mech. B/Fluids*, **56**, 178–187, 2016.

[2] Cooper, A.J., Harris, J.H., Garrett, S.J., Ozkan, M. and Thomas, P.J., The effect of anisotropic and isotropic roughness on the convective stability of the rotating disk boundary layer, *Physics of Fluids*, **27**, 014107, 2015.

[3] Denier, J. P. and Hewitt, R. E., Asymptotic matching constraints for a boundary-layer flow of a power-law fluid, *J. Fluid Mech.*, **518**, 261–279, 2004.

[4] Gajjar, J.S.B., Nonlinear critical layers in the boundary layer on a rotating disk, *Journal of Engineering Mathematics*, **57**, 205-217, 2007.

[5] Garrett, S.J., Cooper, A.J., Harris, J.H., Ozkan, M. and Segalini, A., On the stability of von Kármán rotating-disk boundary layers with radial anisotropic surface roughness, *Physics of Fluids*, **28**, 014104, 2016.

[6] Griffiths, P. T., Stephen, S. O., Bassom, A. P. and Garrett, S. J., Stability of the boundary layer on a rotating disc for power law fluids, *J. Non-Newton. Fluid*, **207**, 1–6, 2014.

[7] Griffiths, P. T., Garrett, S. J. and Stephen, S. O., The neutral curve for stationary disturbances in rotating disk flow for power-law fluids, *J. Non-Newton. Fluid*, **213**, 78–81, 2014.

[8] Griffiths, P. T., Flow of a generalised Newtonian fluid due to a rotating disk, *J. Non-Newton. Fluid*, **221**, 9–17, 2015.

[9] Hall, P., An asymptotic investigation of the stationary modes of instability of the boundary layer on a rotating disc, *Proc. R. Soc. Lond. A*, **406**, 93–106, 1986.

[10] Rajagopal, K. R., Flow of viscoelastic fluids between rotating disks, *Theor. Comp. Fluid Dyn.*, **3**, 185–206, 1992.

[11] Sahoo, B. and Sharma, H. G., Effects of partial slip on steady Von Kármán flow and heat transfer of a non-Newtonian fluid, *Bull. Braz. Math. Soc.*, **38**, 595–609, 2007.